Available online at www.sciencedirect.com
ScienceDirect
Ceramics International 37 (2011) 1277–1283
CERAMICS INTERNATIONAL
www.elsevier.com/locate/ceramint

Reaction kinetics and ablation properties of C/C–ZrC composites fabricated by reactive melt infiltration

Yiguang Wang *, Xiaojuan Zhu, Litong Zhang, Laifei Cheng

National Key Laboratory of Thermostructure Composite Materials, Northwestern Polytechnical University, Xi'an 710072, Shannxi, PR China

Received 30 August 2010; received in revised form 15 September 2010; accepted 3 December 2010
Available online 21 January 2011

Abstract

Carbon/carbon–zirconium carbide (C/C–ZrC) composites were prepared by reactive melt infiltration. Carbon fiber felt was firstly densified by carbon using chemical vapor infiltration to obtain a porous carbon/carbon (C/C) skeleton. The zirconium melt was then infiltrated into the porous C/C at temperatures higher than the melting point of zirconium to obtain C/C–ZrC composites. The infiltration depth as a function of annealing temperature and dwelling time was studied. A model based on these results was built up to describe the kinetic process. The ablation properties of the C/C–ZrC were tested under an oxyacetylene torch and a laser beam. The results indicate that the linear and mass ablation rates of the C/C–ZrC composites are greatly reduced compared with C/SiC–ZrB_2, C/SiC, and C/C composites. The formation of a dense layer of ZrC and ZrO_2 mixture at high temperatures is the reason for high ablation resistance.

Keywords: Ceramic–matrix composites (CMCs); Environmental degradation; Liquid metal infiltration (LMI)

1. Introduction

C/C composites have many excellent properties such as low density, high specific strength, high thermal conductivity, resistance to thermal shock and ablation [1,2]. These excellent properties render them as potential materials for high temperature applications in nose tips, leading edges, reentry heat shields, and nozzles of solid rocket motors [2,3]. However, advanced space systems require the materials capable of prolonged operation in oxidizing atmospheres above 2000 °C [4]. For example, sharp leading edges for hypersonic vehicles will expose to ultrahigh temperatures (>2200 °C) in oxidizing environments. The combustion temperature of a scramjet propulsion system will reach close to 2700 °C. C/C composites cannot meet the requirements any more because their rapid ablation at the scouring of the ultrahigh temperatures and high pressure flux will seriously limit the whole performance of the vehicles [5]. It is necessary to improve their ablation resistance in ultrahigh temperatures and oxidizing atmosphere.

Refractory carbide/boride ceramics, known as ultrahigh temperature ceramics (UHTCs), can withstand the extreme thermal and chemical environments due to their high melting temperatures, high hardness, and retained strength at high temperatures [6]. Introducing refractory carbide/boride compounds into C/C matrix is one of the widely used methods to improve the ablation resistance of C/C composites. In the last few years, many efforts have been made to develop the C/C–UHTC composites [3,7–11]. Tang et al. [3] introduced ZrB_2, HfC, SiC, and TaC into C/C composites to improve the ablation resistance by using powder infiltration. Li et al. [7] and Tong et al. [8] prepared ZrC doped C/C composites by hot-pressing. Shen et al. [9] introduced ZrC into C/C by immersion of liquid $ZrOCl_2$ precursor. Refractory carbide/boride coatings [10,11] were also fabricated on carbon materials by chemical vapor deposition (CVD). Although these efforts can increase the ablation resistance of C/C composites, the reduction in the erosion of C/C composites is limited. It is because the refractory carbide/boride content in these C/C–UHTC composites is low. For instance, the ZrC in C/C–ZrC composites prepared by Shen et al. [9] was only 4–5 wt%.

Reactive melt infiltration (RMI) has been widely used to introduce a great deal of SiC into C/C matrix to form C/C–SiC composites [12–17]. It is also expected to increase the ZrC

* Corresponding author. Tel.: +86 29 88494914; fax: +86 29 88494620.
E-mail address: wangyiguang@nwpu.edu.cn (Y. Wang).

0272-8842/$36.00
doi:10.1016/j.ceramint.2010.12.002

content in the C/C matrix by this process. However, C/C–ZrC composites fabricated by RMI still have rarely been reported so far. Only Zou et al. [18] reported the microstructural characterization of C/ZrC composites by RMI. In this study, we prepared C/C–ZrC composites by RMI. The kinetics of the infiltration was studied. The ablation properties of the C/C–ZrC composites were investigated using an oxyacetylene torch and a laser beam. The results demonstrate that the introduction of ZrC by RMI into C/C composites greatly increases their ablation resistance.

2. Experimental procedure

3D needled felt was fabricated by a needle-punching technique with alternatively stacked weftless piles (T-300^{TM}, HTA-1000, TOHO, Japan) and short-cut-fiber webs. The fiber volume is about 40%. The needled felts were used as reinforcement of the C/C–ZrC composites.

The as-obtained fiber felt was firstly infiltrated with carbon by chemical vapor infiltration (CVI) to form a porous C/C skeleton. The density of the porous preform is controlled to be 1.4 g/cm^3. The zirconium powder (99.5% purity, Alfa Aesar, Tianjin, China) was molten in a flowing argon gas at temperatures higher than its melting point (1850 °C). The molten zirconium was infiltrated into the preform by capillary forces along the carbon fiber tow, where it reacted with the deposited carbon to form C–ZrC matrix.

The kinetics of RMI for C/C–ZrC composites was determined by measuring the depth of formed ZrC in the composites as a function of infiltration temperature and dwelling time. The depth was measured as the following steps: first, the as-obtained C/C–ZrC composites were coated with epoxy and then cut into halves. The cross-section of the specimen was polished to 1 μm finish. The polished surface was then observed under a secondary electron microscope (SEM, JEOL-6700F, Tokyo, Japan). The depth of ZrC was measured at least five points to obtain an average value.

The ablation properties of C/C–ZrC composites were tested using an oxyacetylene flame and a laser beam. Before the ablation tests, a SiC layer with a thickness of about 60–80 μm was deposited on the C/C–ZrC composites according to [19].

The oxyacetylene flame ablation tests were carried out in a vertically jetted flowing oxyacetylene torch environment. The exposure time under the torch flame was 20 s. At least three samples with a dimension of Φ30 × 5 mm were used in the tests. Further details about the test process were described elsewhere [11]. The temperature distribution on the sample surface was calculated using the FLUENT software based on the method of Gibbs free energy minimization. It was assumed that there was no friction between the flowing gas and equipment tubes. The results showed that the heat flux was about 4200 kW/m^2 (±10% error) and the temperature in the center of the sample was about 3000 °C, which was in accordance with the measured temperature by multiwavelength pyrometer [11,19].

The laser beam used in the laser ablation test was produced by a continuous wave CO_2 laser (ROFIN DC080W, Germany). The laser beam ablation was carried out on different areas of the same sample with a defocusing distance of 60 mm. During the ablation test, the target material was placed in a chamber, which was filled with flowing argon gas. However, the sealing of the chamber is not tight enough so that a small amount of air will enter into the flowing argon gas. Three laser powers of 100, 1000, and 2000 W were selected to vertically irradiate on the materials. The scanning distance of the laser beam is 20 mm with a scanning rate of 2000 mm/min for four cycles. The temperatures of the ablated surface were measured by an infrared thermometer (Raytek MR1SCSF, CA, USA). The ablation depth was measured using SEM.

The phases of composites were analyzed by X-ray diffractometer (XRD, Rigaku D/max-2400, Tokyo, Japan) with Cu Kα radiation. Data were digitally recorded in a continuous scan mode in the angle (2θ) range of 15–80° with a scanning rate of 0.12°/s. The microstructure of the specimens was observed by SEM. The elemental analysis was conducted by energy dispersive spectroscopy (EDS). The density of the samples was measured by the Archimedes method with distilled water.

3. Results and discussion

3.1. Infiltration kinetics of RMI for C/C–ZrC composites

The depth of ZrC as a function of annealing temperature and time was shown in Fig. 1. At 1900 °C, the depth of ZrC grows all the time from 15 min to 60 min though its values are small. With the increase in temperature, the infiltration depth of ZrC increases. However, at high temperatures, the growth of depth by elongation of dwelling time is retarded. For example, the depth is almost constant at 2000°C when the dwelling time is longer than 15 min.

It is known that the depth of ZrC is determined by the infiltration of zirconium melt in the carbon porous preform. According to Poiseuille law [13], the Darcy law [14] and Washburn formula [20] without considering the gravity effect,

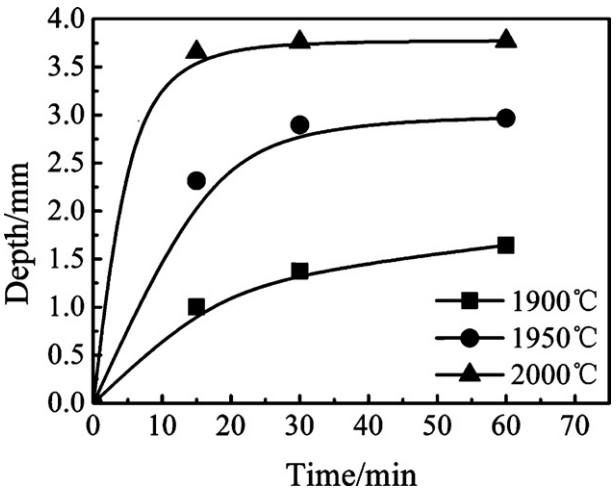

Fig. 1. Infiltration depth of ZrC as a function of annealing temperature and time.

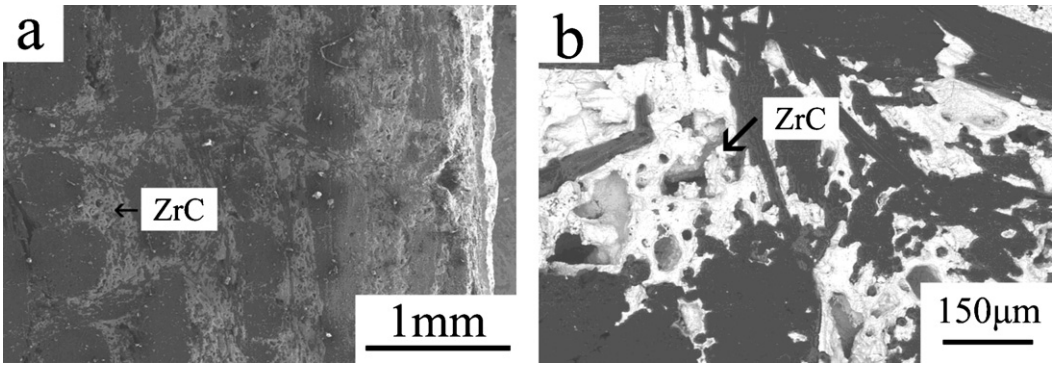

Fig. 2. The cross-sections of C/C–ZrC composites fabricated at 2000 °C for 15 min. (a) 35× and (b) 150×.

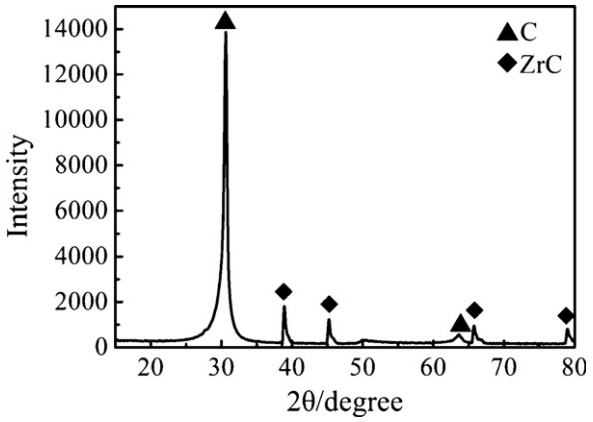

Fig. 3. XRD pattern of C/C–ZrC composites fabricated at 2000 °C for 15 min.

the depth of ZrC can be expressed as follows:

$$\frac{dh}{dt} = \frac{R_t \sigma \cos\theta}{4\eta h} \tag{1}$$

where h is the depth of liquid Zr melt in the preform, t is the annealing time, R_t radius of capillary at t time, σ is the surface tension, θ is wetting angle, and η is viscosity of zirconium melt. The radius of capillary is reduced with the prolongation of annealing time. It is determined by the reaction between zirconium and carbon. According to Adelsberg's study [21], zirconium reacts with carbon to form a ZrC layer quickly and carbon will then diffuse through the layer to grow ZrC. The growth process is controlled by carbon diffusion. Therefore, the radius of capillary as a function of annealing time can be written in the following form:

$$R_t = R_0 - \sqrt{2D_C \frac{M_C \rho_{Zr}}{M_{Zr} \rho_C} t} \tag{2}$$

where R_0 is the radius of pores at the beginning, D_C is the diffusion coefficient of carbon in ZrC, M_C is the mole weight of carbon, M_{Zr} the mole weight of zirconium, ρ_C the density of carbon, and ρ_{Zr} the density of zirconium.

$$\text{Set} \quad A = \sqrt{2D_C B}, \quad B = \frac{M_C \rho_{Zr}}{M_{Zr} \rho_C}$$

Therefore, we can use Yang's results [22] to obtain the kinetics for RMI zirconium in C/C porous preform.

$$h = \sqrt{\frac{c\sigma \cos\theta}{2\eta} \left(R_0 t - \frac{2}{3} A t_2^3 \right)} \tag{3}$$

where c is a constant. Eq. (3) is the same as the kinetic model of RMI silicon when considering carbon or silicon diffusion in the SiC to be the controlling step.

From Eqs. (2) and (3), we obtain the time for sealing pores (t_m), at which h will reach its maximum value (h_m).

$$t_m = \left(\frac{R_o}{A} \right)^2 = \frac{R_0^2}{2D_C} \frac{1}{B} \tag{4}$$

$$h_m = K \sqrt{\frac{R_o^3}{\eta D_C}}, \quad K = \sqrt{\frac{c\sigma \cos\theta}{12B}} \tag{5}$$

At each temperature, the infiltration time is determined by the size of capillary and the diffusion rate of carbon. With the increase in temperature, the carbon diffusion is increased exponentially. The time for sealing pores at 1900 °C can be larger than 60 min, while it is only 15 min at 2000 °C. The infiltration depth however is not only determined by R_0 and diffusion coefficient, but also by viscosity of melt and of course wetting angle and surface tension. Although the infiltration time is shortened at high temperatures, the viscosity of

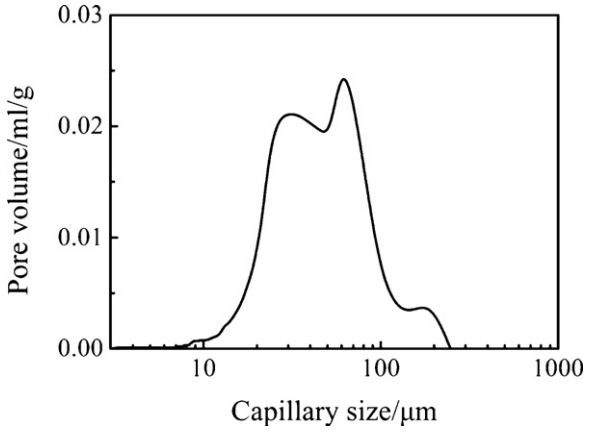

Fig. 4. Pore size distribution in the C/C skeleton.

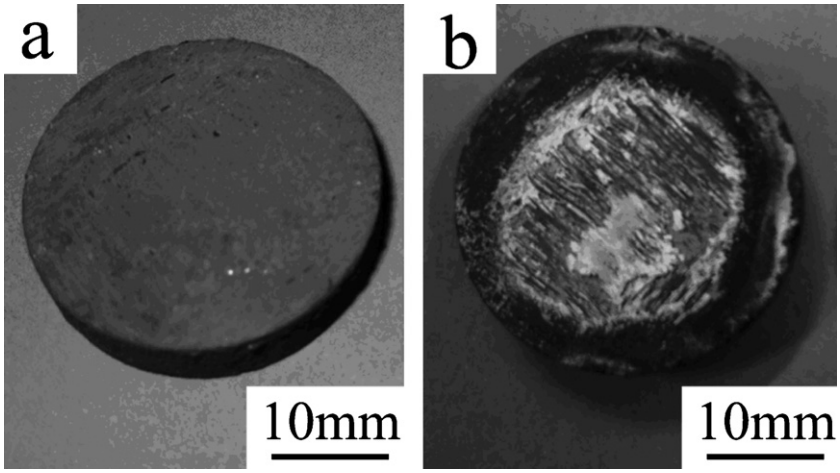

Fig. 5. Macrographic pictures of C/C–ZrC composites. (a) As-obtained C/C–ZrC composites and (b) C/C–ZrC composites ablated by oxyacetylene torch for 20 s.

Table 1
Erosion rates of materials ablated in oxyacetylene flame.

materials	Linear ablation rate mm/s	Mass ablation rate g/s
C/C–ZrC in this study	0.002 ± 0.001	0.004 ± 0.001
C/SiC–ZrB_2 [11]	0.041 ± 0.002	0.0096 ± 0.0005
C/SiC [24]	0.032	0.0052

zirconium will decrease greatly. The infiltration depth can be higher than that at low temperatures. In order to control the depth of ZrC in the final composites, the annealing temperature, dwelling time, and the initial density of C/C porous preform (R_0) should be considered coordinately.

3.2. Microstructure of C/C–ZrC composites

Fig. 2 shows a typical cross-section of C/C–ZrC composites. As can be seen, ZrC is formed deeply along the direction of 3D acupunctures. The generated ZrC is dense and seals the pores inside the composites. The distribution of ZrC is uneven, which is caused by the pores' distribution in C/C porous preform.

The XRD pattern of C/C–ZrC (Fig. 3) indicates that the phases in the composites are carbon and ZrC. As we know, molten silicon into C/C preform by RMI to form C/SiC composites leads to the residual silicon in the final composites, which will deteriorate the high temperature properties of the composites. Unlike silicon infiltration process, no residual zirconium can be found in the final composites.

From the phase diagrams of Zr–C and Si–C, it is learned that the carbon concentration for SiC formation is 50 atm%, 38.5 atm% for ZrC. According to the lever principle, the residual zirconium in RMI C/ZrC is much less than the residual silicon in RMI C/SiC [23]. On the other hand, the carbon diffusion through ZrC layer at high temperatures is fast. As indicated by Adelsberg et al. [21], the growth rate of ZrC layer by carbon diffusion at the temperature of 2000 °C is about $10 \times \sqrt{t}$ μm/min. The distribution of apertures in the porous C/C preform (Fig. 4) indicates that the capillary diameter is mainly in the range of 20–80 μm. It can be calculated that the zirconium in the apertures can be completely transferred to ZrC in 16 min. Therefore, the fast diffusion of carbon and the low carbon concentration for ZrC formation are the reasons why there is no detectable residual zirconium in the final C/C–ZrC composites.

3.3. Ablation properties of C/C–ZrC composites

3.3.1. The oxyacetylene flame ablation

The dimension change of the samples before and after ablation test was measured to obtain the linear ablation rate. The mass ablation rate was determined by the weight change of the samples before and after ablation. The results are listed in Table 1. As can be seen, the linear ablation rate of C/C–ZrC composites is about an order lower than those of C/SiC–ZrB_2 and C/SiC composites [11,24].

The macrographic pictures of C/C–ZrC before and after ablation test are shown in Fig. 5. A white layer can be found on the ablated surface of C/C–ZrC composites. XRD pattern of the ablated samples (Fig. 6) indicates that the white layer consists of a mixture of monoclinic–ZrO_2 and tetragonal–ZrO_2.

The morphologies of the ablated C/C–ZrC composites were shown in Fig. 7. At the brim region of the ablated sample (Fig. 7a), the coated SiC was not totally destroyed. According to the previous studies [11,19], the temperature at the brim

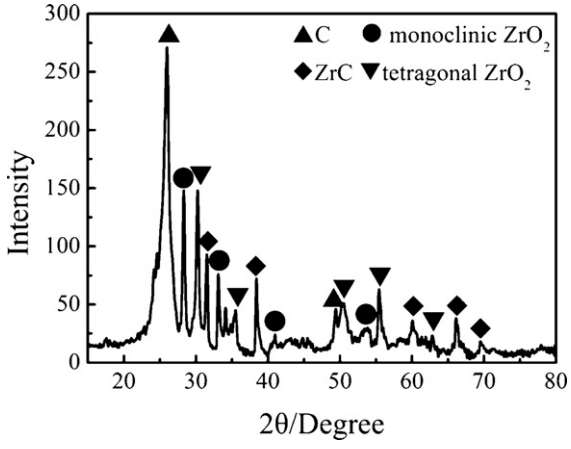

Fig. 6. XRD pattern of the ablated surface in oxyacetylene flame.

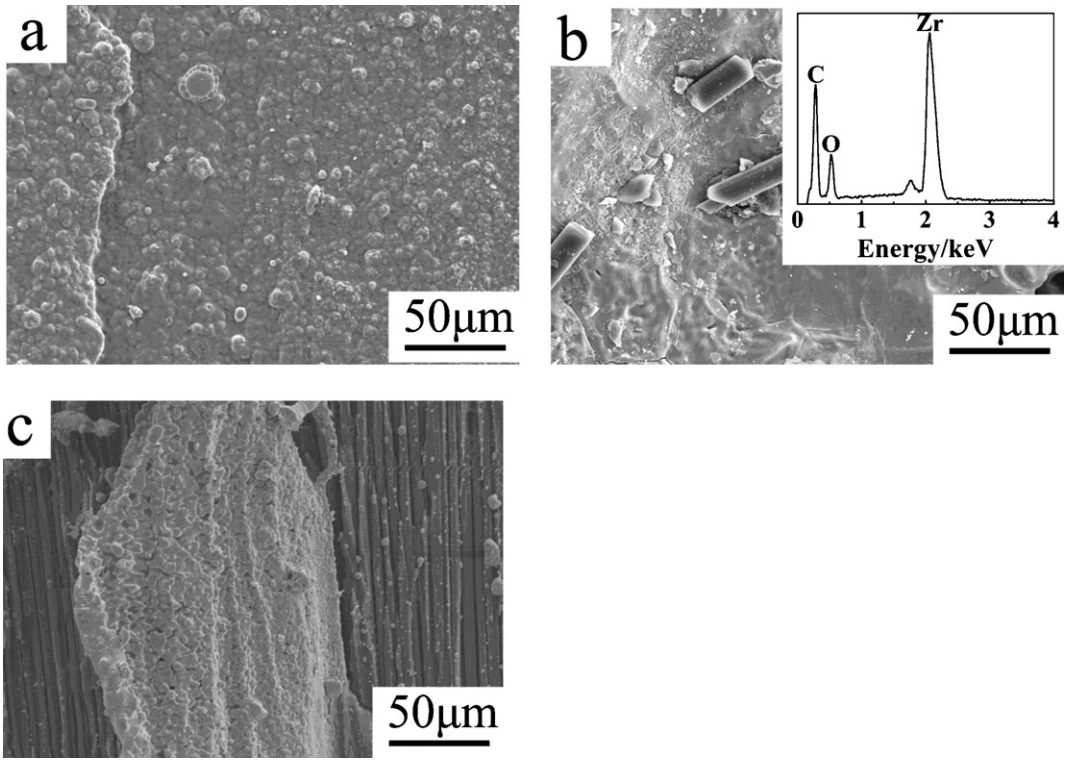

Fig. 7. Morphologies of the ablated surface in oxyacetylene flame. (a) The brim region; (b) the center region, with EDS pattern of the surface; and (c) the region near to the ablation center.

region is about 1700–1800 °C, at which SiC coating can resist the ablation by forming a protective silica layer. At the center of the ablated sample (Fig. 7b), there is a glass-like protective layer. EDS analysis (Fig. 7b) indicates the compositions in this region are zirconium, carbon and oxygen. It can be deduced that the glass-like layer is a mixture of ZrC and ZrO_2. During the ablation process, ZrC will react with oxygen in the flowing gas to form ZrO_2. The center of the ablated sample has the highest temperature of about 3000 °C [17], at which ZrO_2 and ZrC can be sintered together to form a dense layer. The dense layer can resist the ultrahigh temperature scouring of oxyacetylene flame. At the region near to the ablated center, the temperatures are in the range of 2000–2700 °C, much lower than that at the center. However, the surface looks like to be severely damaged (Fig. 7c): there is no or less ZrO_2 on the surface and a lot of ZrC and fibers directly expose to the ablation flame. At the temperature range of 2200–2700 °C, oxygen in the ablation flame will react with ZrC to form ZrO_2. It is believed that the formed ZrO_2 can isolate the heat flux and retard the oxygen to react with the carbon and ZrC matrix. The ablation resistance is thus enhanced. However, when it cools down, ZrO_2 will transform from tetragonal phase to monoclinic phase, which leads to a large volume change. ZrO_2 will spall off the ablated surface. This is the reason why the ZrC and fibers are uncovered near to the ablated center.

The ablation includes two processes, named chemical ablation and mechanical erosion. Chemical ablation refers to the chemical reactions between the composites and the oxidizing atmosphere. The mechanical erosion is the exfoliation of the carbon fibers and matrix by the shearing forces resulted from the flame with high temperature, high velocity, and pressure [25,26]. The formed ZrO_2 or mixture of ZrO_2 and ZrC at high temperature can serve as a barrier to retard the oxygen diffusion. The generated ZrO_2 itself is an excellent thermal barrier material, which can isolate heat flux, reducing the evaporation loss. These characteristics can improve the chemical ablation resistance of C/C–ZrC composites. C/C–ZrC composites also show excellent mechanical erosion resistance at temperatures higher than 2700 °C due to the tightly pinned ZrC matrix and the formed protective layer of ZrC and ZrO_2 mixture. However, at the temperature range of 1800–2700 °C, the formed protective ZrO_2 layer will spall off during cooling down. This problem will be considered in the future study.

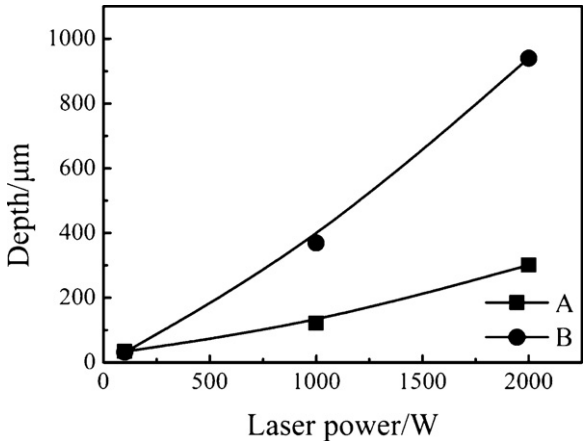

Fig. 8. Ablation depth of C/C–ZrC and C/C composites as a function of laser power. (A) C/C–ZrC composite and (B) C/C composite.

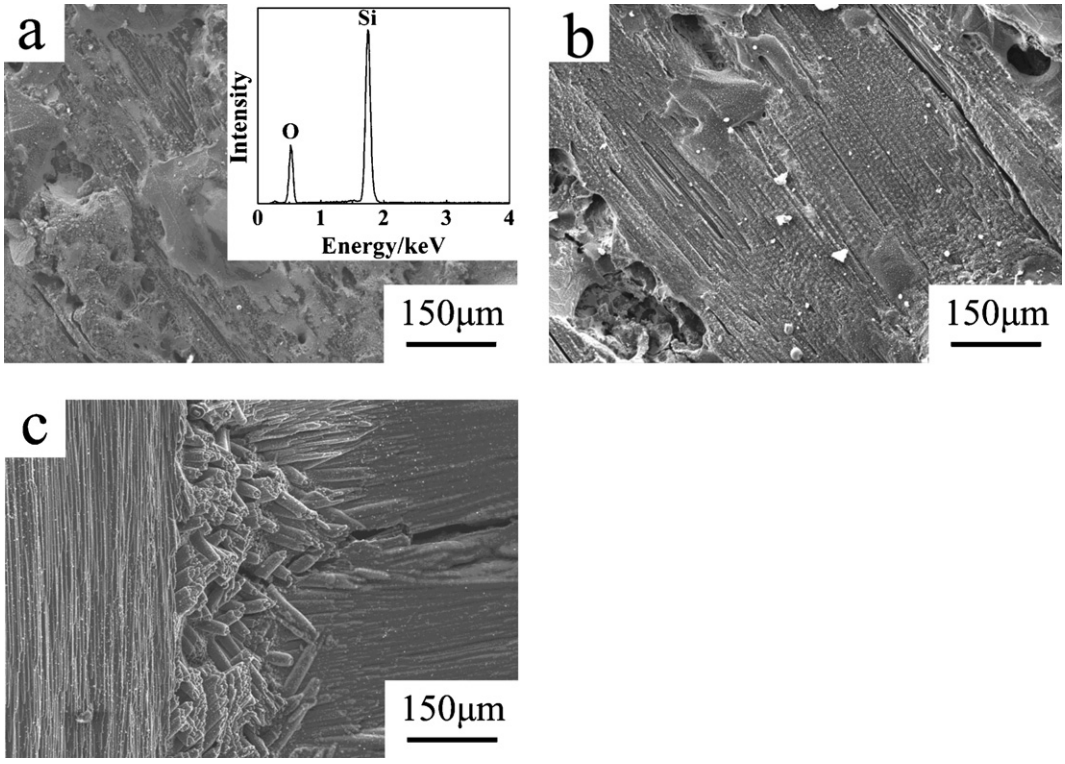

Fig. 9. Surface morphologies of the laser ablated samples. (a) 100 W, with EDS pattern of the surface; (b) 1000 W; (c) 2000 W.

3.3.2. The laser ablation

The ablation depth as a function of laser power for C/C and C/C–ZrC composites is shown in Fig. 8. As can be seen, the ablation depth increases with the increase in laser power, and ZrC can greatly reduce the ablation of C/C composites.

The surface morphology of the sample ablated in 100 W is shown in Fig. 9a. EDS analysis indicates that the compositions at the surface are Si and O. The main phase after 100 W laser ablation is believed to be SiO_2. When the laser power is low, the temperature on the surface is less than 1800 °C. In this temperature range, the SiC can resist the oxidizing ablation environments by forming a dense silica layer on the surface.

The laser power of 1000 W can produce a high temperature on the surface of composites. As indicated by the pyrometer, the temperature is about 3000 °C. At this temperature, SiC layer will be eroded away and a mixture of ZrO_2 and ZrC is formed (Fig. 9b). The mixture layer can act as a protective layer to reduce the ablation of composites.

When the laser power increases to 2000 W, the temperatures on the surface of composites are beyond the testing range of pyrometer. The temperature is far beyond 3000 °C. At this temperature, protective layer of ZrO_2 and ZrC will be eroded away. In this situation, only fibers can be observed on the surface of ablated samples (Fig. 9c).

4. Conclusions

C/C–ZrC composites were fabricated by RMI zirconium melt into porous C/C preform. The kinetics of infiltration was studied. A mathematic model based on the carbon diffusion was proposed. The effects of density of porous C/C composites, annealing temperature and dwelling time on the final products were discussed based on this model.

The microstructure of the obtained C/C–ZrC composites was studied. There is no detectable residual zirconium by XRD, which is due to the fast diffusion of carbon and low carbon concentration for ZrC formation. Because of no residual melt inside, the C/C–ZrC composites will have good high-temperature properties.

The ablation properties of C/C–ZrC composites were studied by oxyacetylene flame and laser beam. The results indicate that C/C–ZrC composites have excellent ablation resistance at high temperatures.

Acknowledgements

This work is financially supported by the Chinese Natural Science Foundation (Grant # 90716023), the Research Fund of State Key Laboratory of Solidification Processing (NWPU) (Grant # 21-TP2007), and ‘‘111’’ project.

References

[1] E. Fitzer, L.M. Manocha, Carbon Reinforcements and Carbon/carbon Composites, Springer, Berlin, 1998, pp. 250–319.
[2] G. Savage, Carbon–carbon Composites, Chapman & Hall, London, 1993, pp. 331–357.
[3] S.F. Tang, J.Y. Deng, S.J. Wang, W.C. Liu, K. Yang, Ablation behaviors of ultra-high temperature ceramic composites, Mater. Sci. Eng. A 465 (2007) 1–7.
[4] W.G. Fahrenholtz, G.E. Hilmas, Future ultrahigh temperature materials. UHTM Workshop Draft Report NSF-AFOSR Joint Workshop on Future Ultra-High Temperature Materials, 2004.

[5] G.F. D'Aleio, J.A. Parker, Ablative Plastics, Marcel Dekker, New York, 1971, pp. 5–7.
[6] S.N. Karlsdottir, J.W. Halloran, Rapid oxidation characterization of ultra-high temperature ceramics, J. Am. Ceram. Soc. 90 (2007) 3233–3238.
[7] X.T. Li, J.L. Shi, G.B. Zhang, H. Zhang, Q.G. Guo, L. Liu, Effect of ZrB_2 on the ablation properties of carbon composites, Mater. Lett. 60 (2006) 892–896.
[8] Q.F. Tong, J.L. Shi, Y.Z. Song, Q.G. Guo, L. Liu, Resistance to ablation of pitch-derived ZrC/C composites, Carbon 42 (2004) 2495–2500.
[9] X.T. Shen, K.Z. Li, H.J. Li, H.Y. Du, W.F. Cao, F.T. Lan, Microstructure and ablation properties of zirconium carbide doped carbon/carbon composites, Carbon 48 (2010) 344–351.
[10] Y.G. Wang, Q.M. Liu, J.L. Liu, L.T. Zhang, L.F. Cheng, Deposition mechanism for chemical vapor deposition of zirconium carbide coatings, J. Am. Ceram. Soc. 91 (2008) 1249–1252.
[11] H.B. Li, Y.G. Wang, L.T. Zhang, L.F. Cheng, Ablation resistance of different coating structures for C/ZrB_2–SiC composites under oxyacetylene torch flame, Int. J. Appl. Ceram. Technol. 6 (2009) 145–150.
[12] W. Krenkel, Carbon fibre reinforced ceramic matrix composites for high performance structures, Int. J. Appl. Ceram. Technol. 1 (2004) 188–200.
[13] W.B. Hillig, Melt infiltration approach to ceramic matrix composites, J. Am. Ceram. Soc. 71 (1988) 96–99.
[14] R.P. Messner, Y.M. Chiang, Liquid-phase reaction-bonding of silicon carbide using alloyed silicon–molybdenum melts, J. Am. Ceram. Soc. 73 (1990) 1193–1200.
[15] O. Chakrabarti, P.K. Das, Reactive infiltration of Si–Mo alloyed melt into carbonaceous preforms of silicon carbide, J. Am. Ceram. Soc. 83 (2000) 1548–1550.
[16] Y.M. Chiang, R.P. Messner, C.D. Terwilliger, Reaction-formed silicon carbide, Mater. Sci. Eng. A 144 (1991) 63–74.
[17] H. Zhou, R.N. Singh, Kinetics model for the growth of silicon carbide by the reaction of liquid silicon with carbon, J. Am. Ceram. Soc. 78 (1995) 2456–2462.
[18] L.H. Zou, N. Wali, J.M. Yang, N.P. Bansal, Microstructural development of a C_f/ZrC composite manufactured by reactive melt infiltration, J. Eur. Ceram. Soc. 30 (2010) 1527–1535.
[19] Y.G. Wang, W. Liu, L.F. Cheng, L.T. Zhang, Preparation and properties of 2D C/ZrB_2–SiC ultra high temperature ceramic composites, Mater. Sci. Eng. A 524 (2009) 129–133.
[20] E.W. Washburn, The dynamics of capillary flow, Phys. Rev. 17 (1921) 273–283.
[21] L.M. Adelsberg, L.H. Cadoff, J.M. Tobin, Kinetics of the zirconium–carbon reaction at temperatures above 2000 °C, Metall. Mater. Trans. 236 (1966) 973–977.
[22] J. Yang, O.J. Ilegbusi, Kinetics of silicon metal alloy infiltration into porous carbon, Composite A 31 (2000) 617–625.
[23] R.V. Sara, The system zirconium–carbon, Am. Soc. Met. 48 (1965) 243–247.
[24] J.J. Nie, Y.D. Xu, L.T. Zhang, L.F. Cheng, J.Q. Ma, Ablation properties of three dimensional needled C/SiC composites by the chemical vapor infiltration, J. Chin. Ceram. Soc. 34 (2006) 1238–1242.
[25] J.M. Su, Research and application of bulk-needled-felt reinforced carbon composites throat, New Carbon Mater. 12 (1997) 46–49.
[26] J. Yin, X. Xiong, H.B. Zhang, B.Y. Huang, Microstructure and ablation performances of dual-matrix carbon/carbon composites, Carbon 44 (2006) 1690–1694.